DAHLGREN DIVISION
NAVAL SURFACE WARFARE CENTER
Dahlgren, Virginia 22448-5100

NSWCDD/TR-02/112

RFC VALIDATION – STATISTICAL ON-TIME COMPARISON WITH IN-SITU METHODS

BY ROBERT PAWLAK AND JANET STAPLETON
NSWCDD

WILLIAM THORNTON
LOCKHEED MARTIN CORPORATION
TACTICAL SYSTEMS DIVISION
DAHLGREN, VIRGINIA

THEATER WARFARE SYSTEMS DEPARTMENT

NOVEMBER 2002

REPORT DOCUMENTATION PAGE

Form Approved
OMB No. 0704-0188

1. AGENCY USE ONLY (Leave blank)	2. REPORT DATE	3. REPORT TYPE AND DATES COVERED
	November 2002	Final

4. TITLE AND SUBTITLE

RFC VALIDATION – STATISTICAL ON-TIME COMPARISON WITH IN-SITU METHODS

5. FUNDING NUMBERS

6. AUTHOR(s)

Robert Pawlak and Janet Stapleton (NSWCDD)
William Thornton, Lockheed Martin Corp., Tactical Systems Division

7. PERFORMING ORGANIZATION NAME(S) AND ADDRESS(ES)

Commander
Naval Surface Warfare Center
Dahlgren Division (Code T41)
17320 Dahlgren Road
Dahlgren, VA 22448-5100

8. PERFORMING ORGANIZATION REPORT NUMBER

NSWCDD/TR-02/112

9. SPONSORING/MONITORING AGENCY NAME(S) AND ADDRESS(ES)

10. SPONSORING/MONITORING AGENCY REPORT NUMBER

11. SUPPLEMENTARY NOTES

12a. DISTRIBUTION/AVAILABILITY STATEMENT

Approved for public release; distribution is unlimited.

12b. DISTRIBUTION CODE

13. ABSTRACT (Maximum 200 words)

The ability to extract a refractivity profile from in-situ data is a valuable capability for today's radar systems. To date, most investigations have centered upon the use of ancillary sensors to accomplish this task, with varying degrees of success. The purpose of this paper is to quantify the performance of an approach that does not require any ancillary sensors. The results show that under certain conditions, this approach yields results comparable to those obtained from in-situ data collected via rocketsonde, but in its current form, it cannot yet compete with helicopter-derived profiles.

14. SUBJECT TERMS

Refractivity from Clutter (RFC) Algorithm, radar, refractivity profile, in-situ data

15. NUMBER OF PAGES

40

16. PRICE CODE

17. SECURITY CLASSIFICATION OF REPORT	18. SECURITY CLASSIFICATION OF THIS PAGE	19. SECURITY CLASSIFICATION OF ABSTRACT	20. LIMITATION OF ABSTRACT
UNCLASSIFIED	UNCLASSIFIED	UNCLASSIFIED	UL

NSN 7540-01-280-5500

Standard Form 298 (Rev 2-89)
Prescribed by ANSI std. Z39-18
298-102

FOREWORD

For several years, the Naval Surface Warfare Center, Dahlgren Division (NSWCDD), Dahlgren, Virginia (T44) has conducted research, testing, and analysis to better understand the microwave radio frequency propagation environment over the ocean. These investigations have indicated significant value in being able to extract a refractivity profile from radar clutter data. The purpose of this paper is to quantify the performance of such a method, dubbed the "Refractivity from Clutter Algorithm," or RFC. This algorithm was proposed by Mr. Ted Rogers of the Space and Naval Warfare Systems Command San Diego, who also provided the RFC results used in the analysis.

This report has been reviewed by Robert Headley, Branch Head, T44, Jim Mims, Branch Head, T41, and Thomas Kimbrell, Division Head, T40.

If there are any questions concerning this report, they can be forwarded to Robert J. Pawlak, Code T41, NSWCDD.

Approved by:

BARRY L. DILLON, Head
Theater Warfare Systems Department

CONTENTS

APPENDICES

ILLUSTRATIONS

TABLES

INTRODUCTION

This paper is concerned with quantifying the performance of the RFC algorithm, which is discussed in Reference 1, solely under surface-based ducting (SBD) conditions. The scope of the analysis was limited to SBD cases because the RFC algorithm relies partially on the presence of ducted clutter in the radar return, which is a common phenomena on days in which SBD conditions occur. Furthermore, there has been little study of the RFC algorithm's performance on SBD days.

In theory, it would be extremely valuable to have truth data for comparison with the output of the RFC algorithm. Unfortunately, directly instantaneously collected and perfectly measured time, height and range coincident radar and path loss data *does not exist*. However, the Wallops Island 2000 data set, in which fairly exhaustive microwave and atmospheric data were collected, is the data set that comes closest. The analysis approach taken in this report accounts for the fact that there is no source of "perfect" truth data, and as such, test statistics based on means, or medians are employed, in recognition of the fact that there are errors involved in the measurement process.

The Wallops Island 2000 microwave propagation experiments employed various atmospheric and oceanographic sensing systems. Thus it follows that there were multiple approaches to refractivity profile estimation examined in this effort. All took various amounts of time, and each method has its drawbacks. The following list summarizes the approaches that were used.

Helicopter – Both range dependent and range-constant refractive profiles derived from helicopter meteorological measurements were analyzed. Helicopter runs took about 30 minutes each to complete, and there are usually multiple helicopter runs during a particular Microwave Propagation Measurement System (MPMS) data collection session. Meteorological measurements from the helicopter were used to measure relative humidity, altitude, time, temperature and pressure. These measurements were then employed in the Large-Scale Atmospheric Refractivity Range Interpolation (LARRI) model, version 4.0, to produce a refractivity profile. Both the range-dependent and single-profiles was then used with the Tropospheric Electromagnetic Parabolic Equation Routine (TEMPER) version 3.11 to compute propagation factor as a function of height and range.

Refractivity From Clutter (RFC) – This method employs radar clutter returns from the NASA Space and Range Radar (SPANDAR), along with a Bayesian algorithm to estimate the refractive profile. This report only examined the range dependent RFC results, since it was thought that this would allow the best comparison with MPMS direct measurements. RFC clutter data was collected at approximately 15-minute intervals, and the data were processed in batch mode.

Rocketsonde – The measurements made by the rocketsondes were similar to those made by the helicopter. The primary difference between the two systems is that the rocketsondes do not provide range dependent soundings, whereas the helicopters do. Rockets were usually launched when the helicopter was not available. Thus, there were few instances where time-coincident rocketsonde and helicopter data were available.

Standard Atmosphere – The refractivity profile for normal 4/3-earth propagation was computed. This profile was used in TEMPER to compute a coverage diagram of propagation factor vs. range. Or course, this is a very sub-optimal approach for estimating the true refractivity, since this analysis was restricted to surface-based ducting days.

Free Space – In this approach a propagation factor of 0 was used across all range and heights in the field of view. This is clearly not an optimal approach, but it might be somewhat reasonable if there was pre-existing knowledge that a surface based duct was present.

Each of these approaches was compared to MPMS data. This data is obtained from a calibrated RF receiver/transmitter suite that measures pathloss at S, C, and X bands (see Reference 2 for more information). Pathloss was then converted to propagation factor[*]. While the MPMS information is very accurate, it takes some time to collect (nearly 1.5 hours per 30 nmi. run). The propagation factor obtained from the MPMS data was used as a baseline in this report. Barring the availability of the "true" propagation factor, the MPMS data is the data that best corresponds to the "truth".

It should be noted at the outset that not all the results of the analysis are shown in this report. It was not practical to insert the hundreds of figures that were generated; they are included on the CD-ROM.

Additional analysis on the RFC data was also conducted at NSWC. And while the analysis in this paper was concerned with time-matched/on-time data, Reference 3 discusses the effects of time lag on propagation factor predictions.

COMPARISON METHOD

The comparison of results among the various approaches presented some unique problems. Perhaps the most straightforward method is to examine the difference between the propagation factor obtained from MPMS measurements, and the approach in question. This has the advantage of being comparatively easy to implement, and is fairly understandable by a broad audience. However, the drawback of a "micro-level" comparison such as this is that there may be instances where it might indicate poor performance, even though the approach in question may have adequately represented the propagation environment. This can happen when large propagation features are shifted, or have minima/maxima that match, but may not be of the proper amplitude.

[*]This data has some dynamic range limitations which were accounted for when computing the statistics

This would seem to indicate that an image or feature-based approach might be worth examining. However, the difficulty with using such a "macro-type" of comparison scheme is that it takes approximately 1.5 hours to complete an MPMS run, and in all likelihood, there are significant variations in the propagation environment while the measurements are being collected. In fact, preliminary analysis (which is partially discussed in Reference 3) indicates that the time constant for a significant change in propagation conditions is on the order of minutes, rather than hours. If future-testing methodologies allowed for a faster data collection time, a valid macro-level comparison would become possible.

Because of these aforementioned difficulties, and the limited time available for competing this analysis, the development of a suitable large-scale performance metric had to be delayed. However, efforts were made to use the proper micro-level metric via an extensive statistical analysis of the data. Visual comparisons were also made via the use of computer-generated animations of the propagation factor as a function of time. In all cases, those runs with good correspondence between coverage diagrams also had good micro level statistics, and vice versa. These animations, and all tables and graphics are available on the CD.

PROCEDURAL DESCRIPTION OF COMPARISON METHOD

A number of statistics were computed for this part of the analysis, which had several phases. The first phase was conducted to determine whether parametric or nonparametric statistics would be used in subsequent phases. Thus, histograms of the difference between the MPMS propagation factor, and the propagation factor for each of the previously discussed refractivity estimation approaches were computed. The differences were computed over data pairs matched in height and range, within a small time window (maximum extent of 15 minutes). If there were multiple corresponding measurements within a 15-minute window, then the measurement with the smallest time difference was used, and the others discarded. This approach is perhaps best understood with the help of Figure 1. In the figure, all the points falling between the two boxes would be examined, with only one point (the one closest to the MPMS measurement), being used to form the difference.

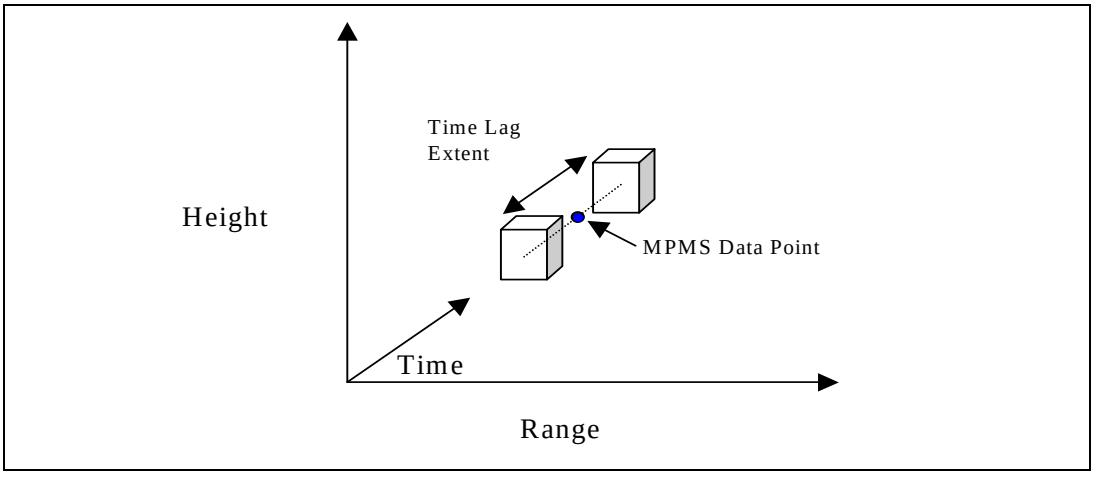

FIGURE 1. PROCEDURE FOR DETERMINING MATCHING DATA POINTS

However, because the MPMS measurements have a limited dynamic range, it was necessary to make sure that propagation factors arising from noise-limited performance were not used in the difference computations. This was done by discarding all the MPMS points that did not pass a threshold test, as follows: First, the propagation loss was computed. A formula for computing the loss is given as follows (from Reference 2):

$$L = PF_{MPMS} + X - 20 * \log_{10}(R * 2665.028)$$

Where L is the loss in dBs, X is the frequency-dependent scaling factor (see Table 1), R is the range in nmi, and PF_{MPMS} is the MPMS propagation factor in dBs. Values for the loss scaling factor and threshold are shown below:

TABLE 1. SCALING FACTORS AND THRESHOLDS FOR SENSITIVITY LIMITS

FREQUENCY BAND	X (DB)	THRESHOLD (DB)
S	57.04	-69.1
C	52.14	-73.1
X	38.63	-80.0

Sets of these differences were then formed for each run. Histograms were computed for each run/set, and summary histograms for the data were constructed across all the runs.

In addition to the histograms, normal probability plots were also constructed. Examples of these plots are shown in Figure 2 through Figure 5. In these figures, different days are represented by different plot symbols and colors. The probability plots indicate large deviations from normality for all the methods examined. If the differences had a perfectly normal distribution, it would be manifested as points clustered very closely about a straight diagonal line on the plot. The observed clusterings indicate that both the helicopter and RFC runs have relatively heavy tails, even in light of the dynamic range limitation of the MPMS data.

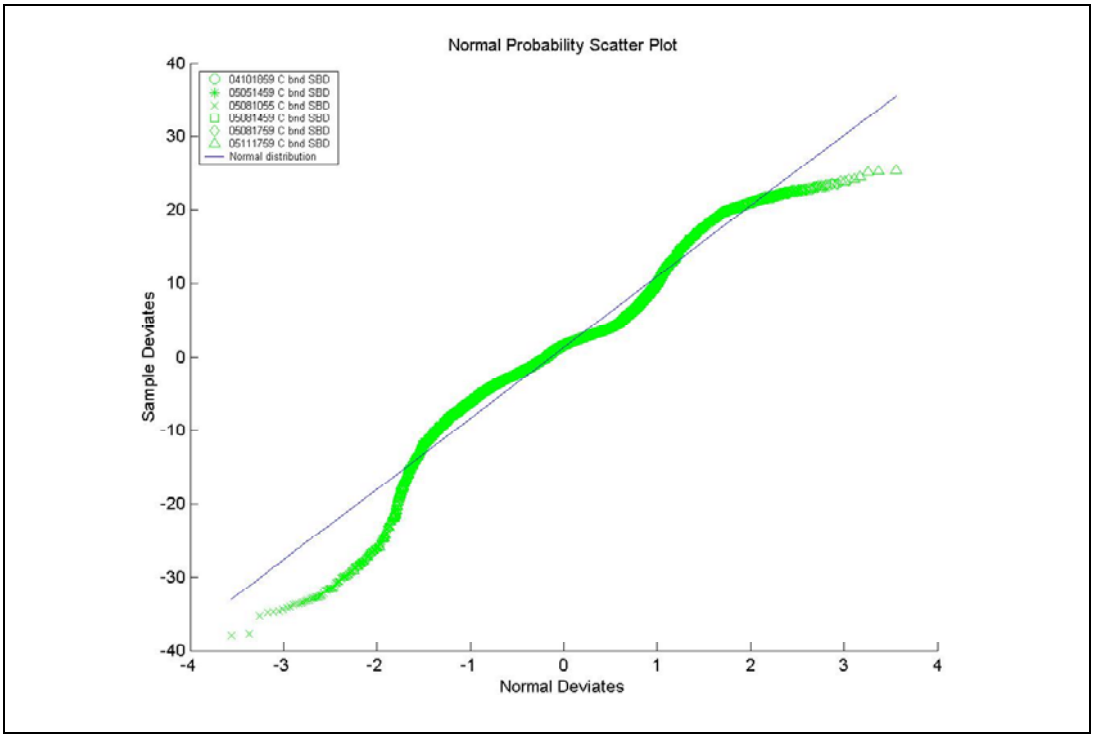

FIGURE 2. NORMAL PLOT ROCKETSONDE, C-BAND

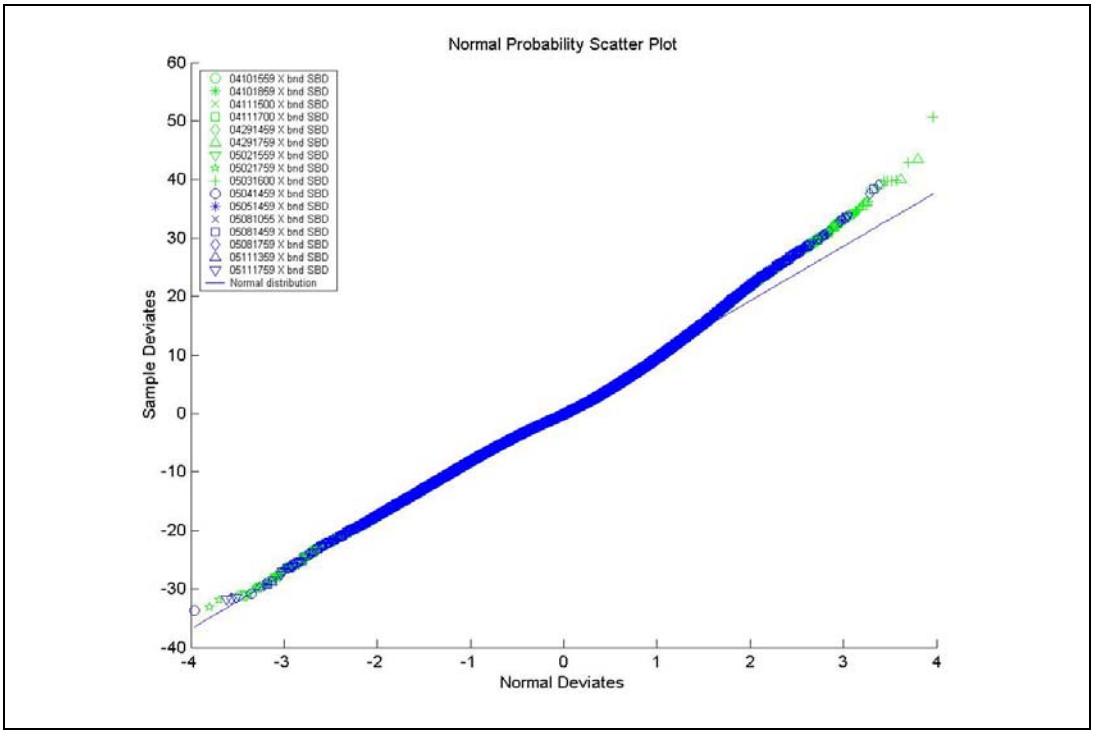

FIGURE 3. NORMAL PLOT RFC, X-BAND

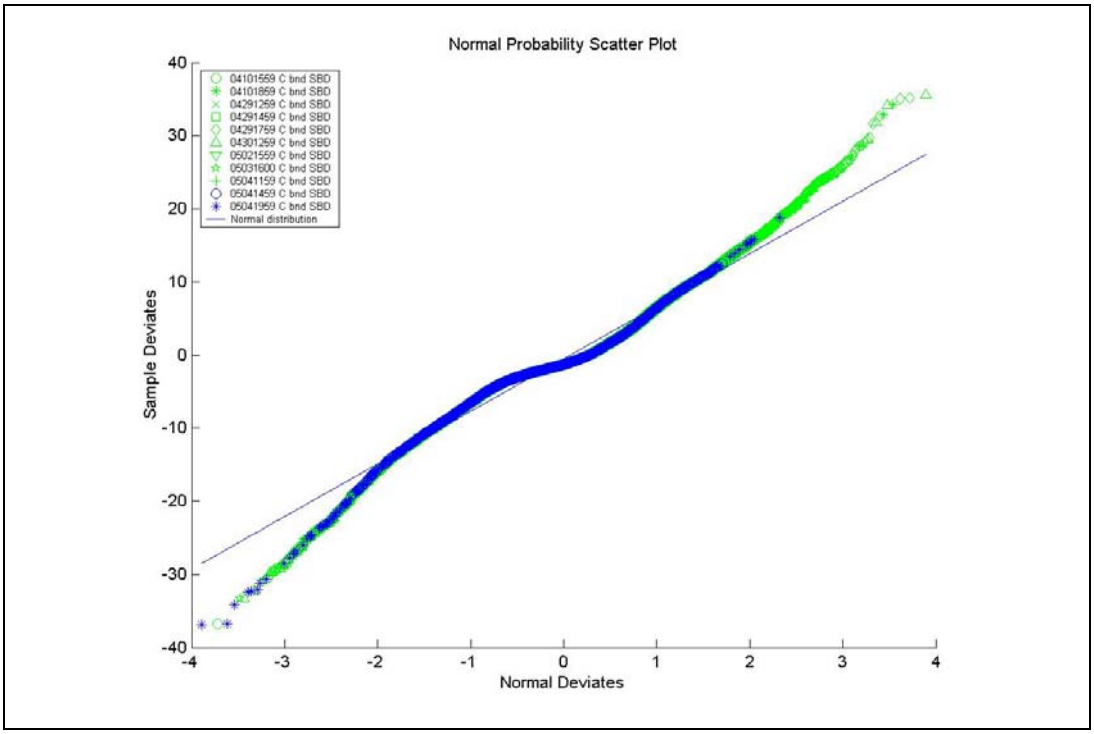

FIGURE 4. NORMAL PLOT RANGE DEPENDENT HELICOPTER, C-BAND

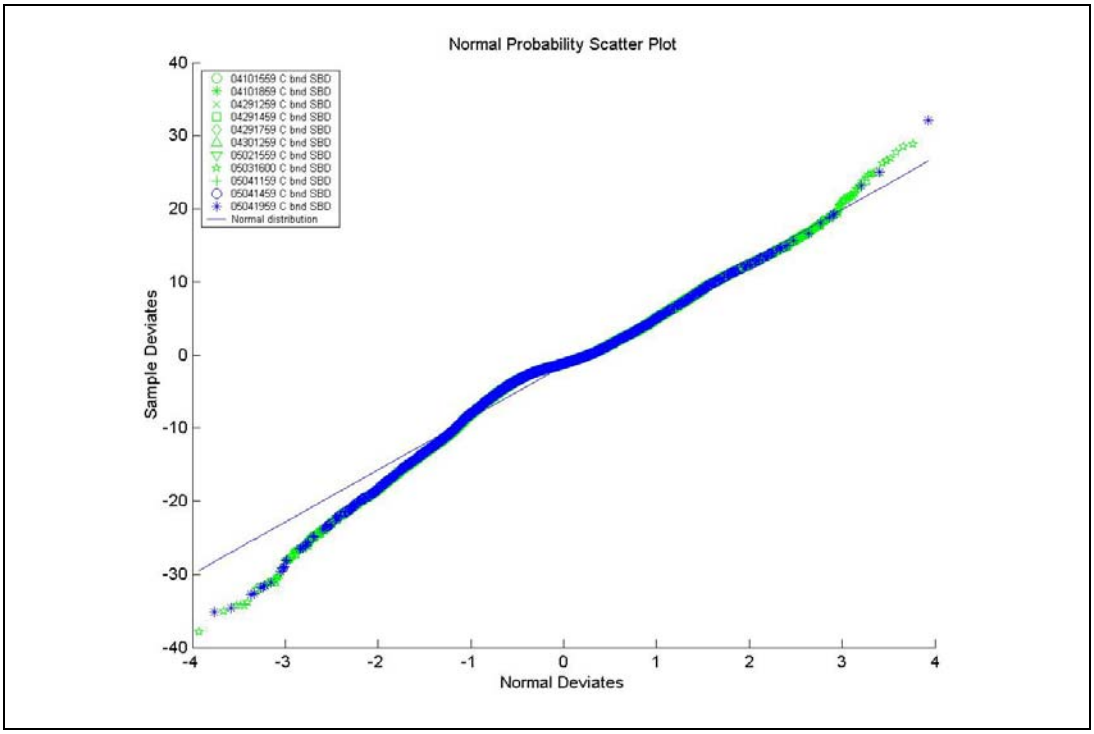

FIGURE 5. NORMAL PLOT SINGLE PROFILE HELICOPTER, C-BAND

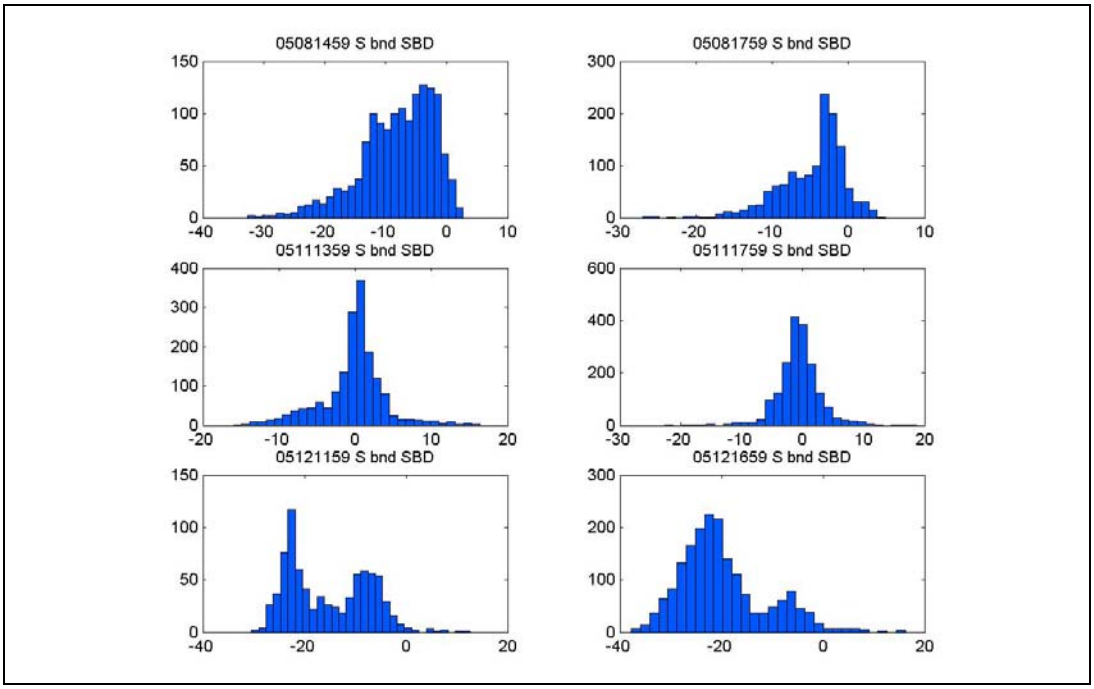

FIGURE 6. SAMPLE HISTOGRAMS OF RFC S-BAND DIFFERENCE DATA

Histograms were also constructed for each method, run, and frequency. The full set of these is on the CD. But for purposes of illustration, the histograms of the difference data for several runs are shown in Figure 6.

The histograms and summary statistics also indicate significant errors for May 12th, which can be seen in Figure 6. Additional examination of this day indicated the absence of surface-based ducting conditions (see Figure 7). Thus, the decision was made to eliminate this day when evaluating the performance of the RFC algorithm. All plots shown in this report (with the exception of Figure 6 and Figure 7) do not contain data from this day.

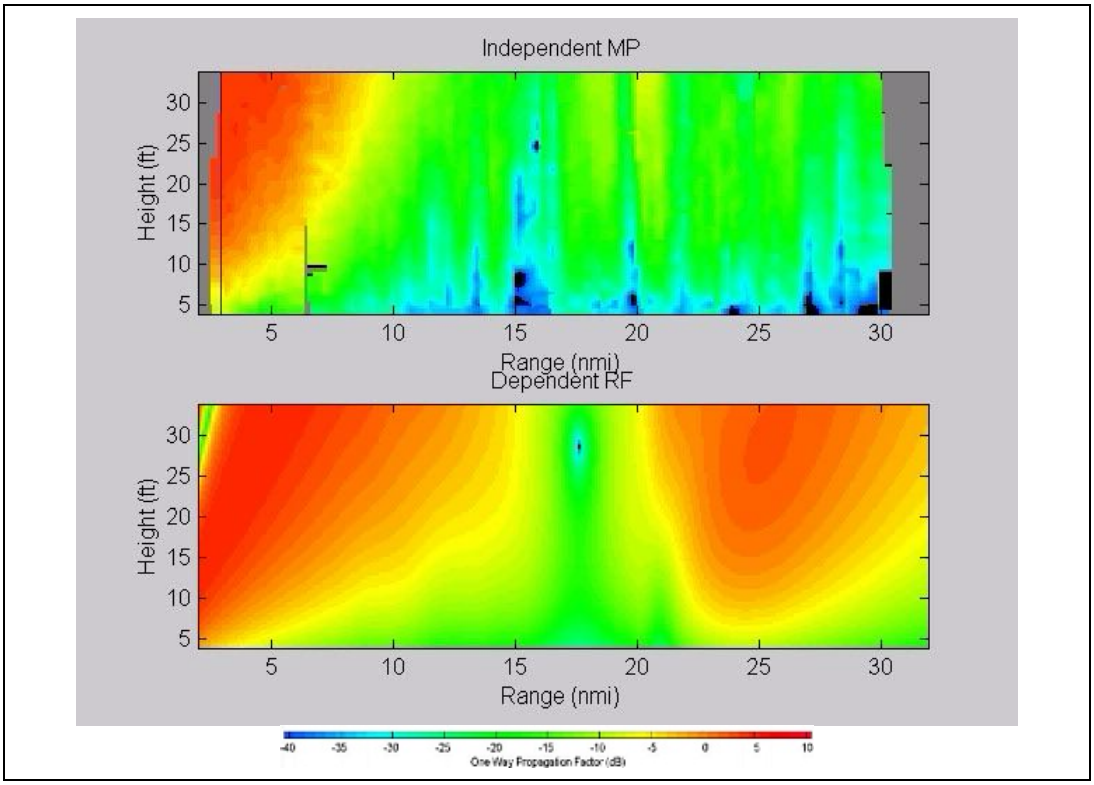

NOTE: Red indicates regions of enhanced propagation, blue indicates decreased propagation.

FIGURE 7. IMAGE PLOT OF COVERAGE DIAGRAM FOR RFC, RUN 05121859

In addition to the histograms and probability plots, skewness and kurtosis were also computed for each run. These were tested against appropriate threshold values to determine if the values could have resulted from a normal distribution. Generally speaking, a large number of these tests failed, these results are shown in Appendix A.

Clearly, the failure of many of the skewness and kurtosis tests, along with the shape of the histograms and normal probability plots for the helicopter, rocket and RFC data, indicate the use of non-parametric statistics for the characterizing the location and scale of the error distributions. To this end, the median and s3 norm (scaled median absolute deviation from the median) should be used when evaluating the performance of any of the methods discussed in this paper. These measures are analogous to the mean and standard deviation for distributions where the normality assumption holds. The following equation details the computation of the s3 norm.

$$s3\langle x\rangle = 1.483 * median\left|x - median(x)\right|$$

Where x is the data for which the norm is to be computed.

Segmentation of Data

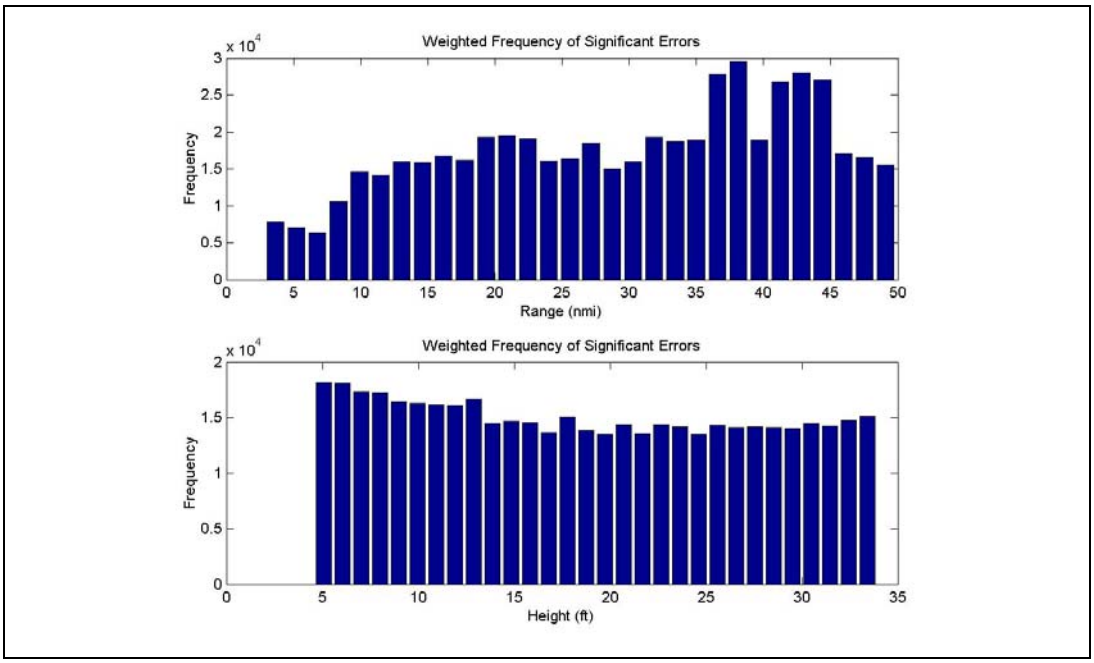

FIGURE 8. FREQUENCY OF SIGNIFICANT ERRORS FOR RFC C-BAND DATA

As part of the analysis, the difference statistics as a function of range were also examined. An example of this analysis is shown in Figure 8. There appears to be little height dependence as far as errors go, across all the approaches. Similar statistics were also computed to look at any range dependence in the errors. Here, it was found that in general, errors for the RFC algorithm do increase with range. Past about 8 nmi, this increase seems significant. One might argue that there is some basis for segmenting the data and looking at those data that are within 8 nmi. When this is done, there is definitely an improvement in the error statistics. However, it should be noted that this is also the case for the other approaches as well. Furthermore, it can be argued that the region beyond 8 nmi is very important, if one is trying to measure track initiation performance.

In this analysis, every effort was made to ensure that valid comparisons were being made among the various data sets. And to the greatest extent possible, all of the data were processed in the same fashion. However, there are some operational limitations associated with performing the in situ measurements. Thus, while it may be possible to employ the RFC algorithm every couple of minutes, the same is not practical with helicopters and rocketsondes. So while the latter may provide superior performance when compared to RFC, it must also be realized that the error for the in situ approaches will, in all likelihood, increase in an operational environment[†]. The error for the RFC approach may even decrease, if a suitably small measurement interval is used for the environmental sensing waveform.

[†] This is due to the larger time and range displacement between the estimated and desired region for the propagation conditions.

Qualitative Comparison of Approaches

The tables in Appendix A show the summary statistics for each of the approaches. It can be seen that the errors for the single profile helicopter, range dependent helicopter, and rocket soundings all have comparable medians and s3 norms. Note that almost none of the in-situ methods can be said to have the same mean as the MPMS measurements.

When the RFC data is examined, it is seen that the results for X-band tend to be better than those for S or C. In some respects, this may be a little counterintuitive, since the radar clutter data was collected at S-band. However, there is clearly some process at work that is causing the predictions at X-band to be superior. Note that the relatively low median and s3 norm at X-band are comparable to the corresponding statistics for the Rocketsonde and Helicopter. One explanation for this behavior could be that there is a smaller set of possible propagation environments for X-band, across most (or all) of the surface based ducts. This would make prediction of environment a bit easier, since the solution space is smaller. For X-band, the median absolute error can be found from consulting Figure 9, and it is easily seen that this value is approximately 5.3 dB. While this is greater than the median absolute error for RFC at S and C bands, there is much less bias (see Table A-3).

It should also be noted that there is significant variability within runs, even at X-band. This can clearly be seen from examining the range-dependent helicopter results for this band.

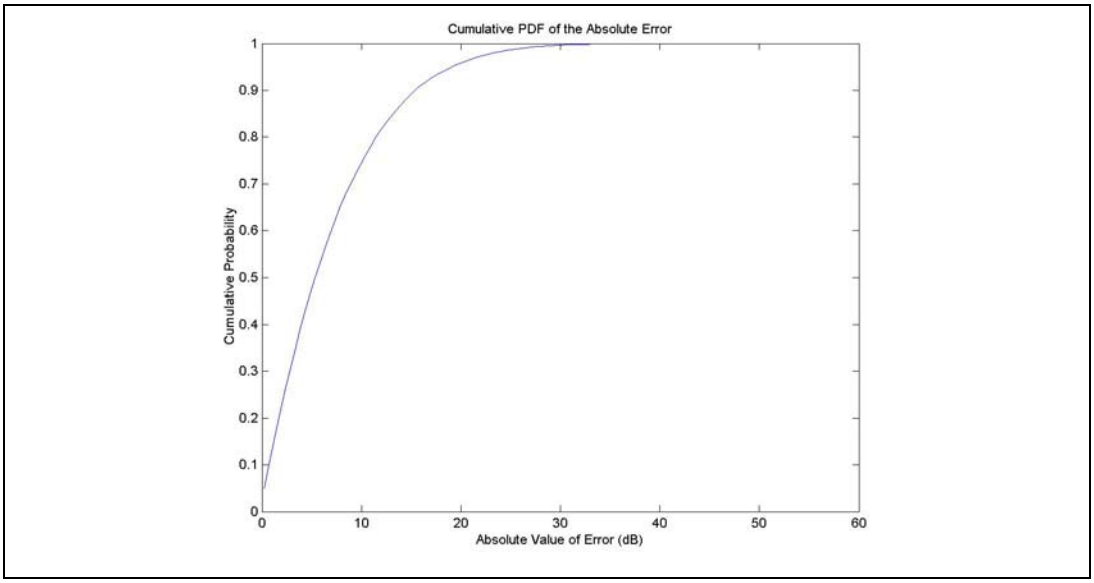

FIGURE 9. CUMULATIVE PDF OF ABSOLUTE ERROR, RFC X-BAND

Additional visual comparison of coverage diagram animations, while not shown in this report (see the CD-ROM), also lead to the conclusion that the RFC predictions are better at X-band. This is because the RFC algorithm at X-band seems to capture most of the salient features of the propagation environment.

The results of the comparison of MPMS data with a prediction based on a 4/3-earth assumption show relatively large median and s3 norms. Since these were all SBD days, this is not a totally unsurprising result. We would expect this kind of poor performance due to the presence of SBD days. Likewise, the median absolute error for this method is also quite high.

The free space results indicate that guessing zero for all the propagation factors is a reasonable approach, especially if no other knowledge is available, and the presence of surface based ducting has been ascertained. The median and s3 norms for the free space approach are on par with the helicopter and rocket soundings. However, this is clearly not an especially clever approach, and it makes no attempt whatsoever to model the salient characteristics of the propagation environment. Whereas one of the other approaches may succeed in showing a slightly shifted horizontal null, for instance, the free space approach would not model this null at all. Thus this final set of statistics illustrates two things: first, that all the approaches have some distance to go before they provide good fine-grain modeling of the propagation environment. Second, these comparable results also show that a strictly "micro-level" approach is inadequate as a sole means of evaluation for these approaches.

Perhaps one of the best ways to summarize the results is to construct a table of the absolute error at the 10^{th}, 50^{th} and 90^{th} percentile points. This is shown in Table 2. More detailed results can be obtained by consulting the individual figures on the CD-ROM. Generally speaking, the results do support the thesis that the RFC results are comparable to those from the rocket. The single and range dependent profiles used by the helicopter corresponded most closely to the MPMS results, of all the approaches that were examined in the report. It can also be seen that the median absolute error is less than about 5 dB about half the time, for the RFC algorithm. From looking at the table, it is apparent that the median absolute error for the X-band RFC data was higher than for C and S bands. However, visual examination of the animations on the CD supports the assertion that the X-band results are better. This is because the median absolute error (like many statistics), does not tell the whole story. Also, comparison of the results in Table A-3 to data in Table A-1 and Table A-2, show that the bias for the RFC X-band predictions is closer to zero than for S or C.

TABLE 2. PERCENTILE POINTS FOR ABSOLUTE ERROR

%	BAND	RFC (DB)	ROCKETSONDE (DB)	RANGE DEPENDENT HELICOPTER (DB)	SINGLE PROFILE HELICOPTER (DB)	FREE SPACE (DB)	STANDARD ATMOSPHERE (DB)
10%	S	0.5	1.1	0.7	0.5	0.8	0.5
	C	0.6	0.9	0.5	0.5	0.8	0.6
	X	0.7	0.8	0.5	0.2	0.8	0.5
50%	S	4.0	5.1	3.4	3.7	4.8	15.7
	C	4.8	3.9	3.5	3.5	4.8	17.7
	X	5.3	4.9	3.7	3.7	3.7	10.9
90%	S	14.3	16.6	10.2	12.2	13.1	51.2
	C	15.9	18.3	12.0	12.3	13.3	55.4
	X	15.4	13.9	11.7	12.3	10.5	51.1

One more thing should also be noted when interpreting the results. The comparisons shown in this report were limited to a small subset of the range and height space, since the physical constraints limited the collection of MPMS data at higher altitudes. While it may be argued that this is the most important region (for some applications), the results should not really be taken out of context, since they might not be predictive of performance at higher altitudes. For instance, the free space approach would definitely have poorer performance above the duct, but this fact is simply not reflected in the data, since there are no MPMS measurements in this regime.

RESULTS OF INFERENTIAL STATISTICS

It was anticipated that the inferential statistics would confirm that the approaches based on in situ measurements would provide unbiased estimates of the propagation factor. Unfortunately, this hypothesis was rejected at a confidence level of 90%. This could be due to a variety of factors, since the models used for these processes are extremely complex, and all of them use TEMPER, which is a very detailed model itself.

The conclusion that can be reached from this phase of the analysis is that none of the approaches provide a statistically unbiased estimate of propagation factor for this set of surface based ducting runs, across all frequencies.

Interestingly, the Rocketsonde comes closest to providing an unbiased estimate. For example, examination of the Wilcoxon test statistic for the Rocketsonde data (Table A-6) to the rest of the tables in the appendix show that this method comes closest to providing unbiased estimates for the propagation factor. In fact, it can be said that the X-band propagation factor estimates from the Rocketsonde are unbiased, since the Wilcoxon statistic falls well within the 90% confidence region. This means that the Rocketsonde approach is likely to result in an estimate of the propagation factor that is neither too high nor too low.

SUGGESTIONS FOR FUTURE STUDY

Accurate prediction of shipboard radar detection, tracking and engagement performance must employ accurate refractivity, sensor and tracker models. The utility of these models is a function of how accurately the firm track range, and possibly other track life stages, are predicted. If enough representative targets are modeled, it should be possible to ascertain the utility of any of the approaches using common statistical techniques. However, this approach to performance evaluation calls for a model of the radar tracker (and specific radar), and will not be applicable to other radar systems.

While the above scheme could result in a performance metric that is highly correlated with the expected gain in utility, there are clearly some issues that need to be resolved before such a study can take place. These issues are surely not insurmountable, but computing an expected utility based on the above will be time and resource intensive.

It might also be fair to conduct the error analysis at time intervals that are more representative of an operational scenario. For instance, it might be better to look at Rocketsonde results from two to three hours away, and compare these to RFC results that might have a maximum separation of one minute.

CONCLUSIONS

The results of this analysis clearly indicate that approaches based on helicopter data are superior to the other approaches, if the only concern is accurate modeling of the propagation environment. The results also indicate that the errors associated with the RFC and Rocketsonde based approaches are comparable. While the median value of the absolute errors are all quite close, the animations, and statistics based on the signed error point to the X-band being a little closer to the MPMS measurements than either the S or C band.

It was also seen that none of the approaches provided a completely unbiased estimate of the propagation conditions under all circumstances, although the Rocketsonde data came closest in this regard.

REFERENCES

[1] Gerstoft, P., L.T. Rogers, W.S. Hodgkiss and G. Rovner, "Refractivity from clutter using global environmental parameters", *Proc. of the International Geoscience and Remote Sensing Symposium*, Sydney, Australia, Jul. 9-13, 2001.

[2] Stapleton, et al, "Radar Propagation Modeling Assessment Using Measured Refractivity and Directly Sensed Propagation Ground Truth – Wallops Island, VA 2000", NSWCDD/ TR-01/132

[3] Stapleton, Thornton, "RFC Validation – Lag Analysis", NSWC White paper, Sept 2002

APPENDIX A

TABLES OF ERROR STATISTICS

Table Notes:

1. Under column heading of 'Data', the date is shown in the format MMDDHHMM, i.e. month, day, hour, and minute.
2. 'Tests Failed' refers to whether that data set failed the skewness and kurtosis tests. Failure of the skewness test is denoted by 's', failure of kurtosis test is designated by 'k'.

TABLE A-1. RFC, S-BAND

DATA	MEAN	STDEV	MEDIAN	S3 NORM	SKEWNESS	KURTOSIS	TESTS FAILED	# SAMPLES
04101559	-1.75	6.30	-1.84	5.84	0.28	0.93	SK	2625
04101859	2.67	2.00	2.16	1.22	0.93	1.50	SK	470
04111500	0.91	6.60	1.98	5.76	-1.92	4.83	SK	1473
04111700	-8.74	8.20	-7.19	7.66	-0.70	0.43	SK	2316
04291459	-1.23	2.77	-1.12	2.86	-0.44	0.42	SK	570
04291759	-4.35	7.95	-2.12	5.51	-0.08	0.46	K	2506
05021559	-1.49	2.83	-1.42	2.35	-0.21	1.21	SK	1030
05021759	-2.14	3.85	-1.80	3.12	-0.30	2.70	SK	2104
05031600	-2.93	9.89	-2.97	10.66	-0.11	0.03	S	3308
05041459	-9.70	5.69	-9.62	6.51	-0.18	-0.68	SK	1571
05051459	-10.51	9.50	-4.64	4.93	-0.59	-1.17	SK	1135
05081055	-11.23	2.48	-11.14	2.66	-0.25	-0.18	S	838
05081459	-8.05	6.01	-7.15	6.01	-0.87	0.70	SK	1453
05081759	-4.65	4.25	-3.44	3.28	-1.15	2.32	SK	1321
05111359	-0.23	4.15	0.25	2.36	-0.21	2.13	SK	1677
05111759	-0.64	3.48	-0.69	2.36	-0.17	5.58	SK	1825
Summary	-4.02	7.55	-2.65	5.89	-0.55	1.21	SK	26222

T-VALUE	-86.37	THRESHOLD	1.64
WILCOXON	-79.80	THRESHOLD	1.64

TABLE A-2. RFC, C-BAND

DATA	MEAN	STDEV	MEDIAN	S3 NORM	SKEWNESS	KURTOSIS	TESTS FAILED	# SAMPLES
04101559	-1.60	8.19	-0.30	6.71	-0.65	1.33	SK	3589
04101859	1.54	3.56	1.24	2.97	-0.00	0.53	K	657
04111500	-0.80	8.22	0.20	8.65	-0.58	-0.22	S	1251
04111700	-8.32	9.97	-6.51	10.55	-0.39	-0.22	SK	2484
04291459	-0.95	3.21	-0.66	3.10	-0.50	0.70	SK	645
04291759	-3.91	7.66	-1.61	4.67	-0.55	0.54	SK	2933
05021559	-0.13	3.66	-0.21	2.51	-0.16	4.06	SK	1085
05021759	-1.44	8.63	-1.28	7.42	-0.57	2.40	SK	2304
05031600	-3.98	10.54	-4.57	9.46	0.43	0.64	SK	3773
05041459	-8.20	7.53	-7.84	8.70	0.10	-0.09		1817
05051459	-8.33	7.81	-6.59	7.90	-0.35	-0.37	SK	1219
05081055	-15.64	4.39	-15.57	4.33	-0.16	-0.05	S	1034
05081459	2.27	6.12	1.94	6.21	0.23	0.21	S	1484
05081759	-0.51	4.96	-1.50	3.21	-0.00	0.58	K	1422
05111359	-0.58	6.64	-0.70	5.91	0.27	0.56	SK	1831
05111759	-1.38	5.58	-1.14	5.09	-0.43	0.77	SK	2032
Summary	-3.36	8.68	-2.08	7.21	-0.36	0.77	SK	29560

T-VALUE	-66.61	THRESHOLD	1.64
WILCOXON	-60.23	THRESHOLD	1.64

TABLE A-3. RFC, X-BAND

DATA	MEAN	STDEV	MEDIAN	S3 NORM	SKEWNESS	KURTOSIS	TESTS FAILED	# SAMPLES
04101559	1.23	10.06	0.65	9.01	0.23	0.41	SK	2646
04101859	-3.52	7.68	-2.86	6.67	-0.24	0.89	SK	483
04111500	1.26	9.00	0.47	8.20	0.32	0.18	S	1255
04111700	-0.16	8.76	-0.80	7.70	0.38	0.44	SK	2344
04291459	0.92	9.61	0.95	7.56	0.11	0.64	K	632
04291759	2.42	9.99	-0.38	8.13	0.62	0.13	S	2771
05021559	-4.01	7.43	-4.23	6.69	-0.09	0.44	K	1094
05021759	-0.72	9.39	-1.71	8.79	0.13	0.35	SK	2177
05031600	3.82	10.00	3.88	7.91	0.02	0.78	K	3423
05041459	-0.92	8.78	-0.45	8.29	0.13	-0.06	S	1676
05051459	-1.31	8.66	-1.32	7.81	0.44	0.67	SK	1134
05081055	0.47	9.65	0.16	8.96	0.59	0.24	S	897
05081459	1.46	9.88	0.76	9.09	0.39	0.17	S	1454
05081759	0.68	7.86	-0.94	5.18	1.11	3.06	SK	1404
05111359	0.44	7.76	0.01	7.50	0.07	0.43	K	1809
05111759	-1.60	8.66	-1.56	8.08	0.11	0.57	SK	2038
Summary	0.56	9.38	-0.16	8.26	0.34	0.59	SK	27237

T-VALUE	9.82	THRESHOLD	1.64
WILCOXON	4.47	THRESHOLD	1.64

TABLE A-4. ROCKETSONDE, S-BAND

DATA	MEAN	STDEV	MEDIAN	S3 NORM	SKEWNESS	KURTOSIS	TESTS FAILED	# SAMPLES
04101859	0.44	3.43	1.40	2.70	-1.09	1.14	SK	231
05051459	-4.93	3.43	-5.98	3.14	0.60	-0.67	S	204
05081055	0.16	9.18	3.89	2.67	-1.57	0.71	SK	748
05081459	-2.60	3.98	-2.54	3.98	-0.44	-0.07	S	1134
05081759	5.37	11.82	1.03	14.06	0.15	-1.59	SK	1198
05111759	2.40	6.83	2.27	9.45	0.17	-1.11	SK	1245
Summary	1.20	8.69	0.49	7.78	0.40	0.30	SK	4760

T-VALUE	9.50	THRESHOLD	1.65
WILCOXON	5.45	THRESHOLD	1.64

TABLE A-5. ROCKETSONDE, C-BAND

DATA	MEAN	STDEV	MEDIAN	S3 NORM	SKEWNESS	KURTOSIS	TESTS FAILED	# SAMPLES
04101859	-0.88	4.14	-0.77	3.58	-1.19	3.95	SK	306
05051459	-1.23	5.23	0.89	4.17	-0.89	-0.37	S	249
05081055	-3.38	12.30	2.48	1.34	-1.56	0.59	SK	877
05081459	2.54	5.86	2.18	6.30	-0.02	-0.27		1141
05081759	5.54	11.37	-0.08	13.56	0.10	-1.55	K	1322
05111759	0.08	8.90	0.10	7.33	0.03	0.50	K	1404
Summary	1.28	9.86	1.62	6.82	-0.47	1.56	SK	5299

T-VALUE	9.45	THRESHOLD	1.65
WILCOXON	11.82	THRESHOLD	1.64

TABLE A-6. ROCKETSONDE, X-BAND

DATA	MEAN	STDEV	MEDIAN	S3 NORM	SKEWNESS	KURTOSIS	TESTS FAILED	# SAMPLES
04101859	6.97	7.47	8.03	6.86	-0.07	0.47		230
05051459	0.70	4.85	0.26	5.30	0.17	-0.74	K	214
05081055	-0.39	6.27	1.96	2.45	-1.65	1.72	SK	805
05081459	-3.32	8.25	-4.47	6.99	0.78	0.99	SK	1122
05081759	3.04	7.24	1.98	6.84	0.13	0.12		1283
05111759	-1.39	9.55	-2.67	8.77	0.27	-0.11	S	1394
Summary	-0.06	8.42	0.02	7.82	0.09	0.20	SK	5048

T-VALUE	-0.52	THRESHOLD	1.65
WILCOXON	-0.91	THRESHOLD	1.64

TABLE A-7. SINGLE -PROFILE HELICOPTER, S-BAND

DATA	MEAN	STDEV	MEDIAN	S3 NORM	SKEWNESS	KURTOSIS	TESTS FAILED	# SAMPLES
04101559	1.62	7.73	2.03	7.99	0.64	0.37	SK	2323
04101859	1.57	5.24	1.68	5.40	0.33	0.62	SK	861
04291259	0.02	3.84	0.58	1.80	-1.72	4.58	SK	1300
04291459	0.38	2.44	0.29	2.68	0.12	0.28	K	1305
04291759	1.24	9.40	3.62	8.91	-0.35	-0.96	SK	2506
04301259	-1.68	7.76	-0.09	6.62	-0.31	0.47	SK	2408
05021559	4.96	5.12	4.54	7.15	0.12	-1.49	K	1048
05031600	-3.14	8.67	-2.02	9.17	-0.21	-0.49	SK	3037
05041159	-0.19	4.41	-0.55	2.00	0.39	2.67	SK	1919
05041459	-3.48	4.45	-2.92	2.80	0.35	2.92	SK	1593
05041959	-3.20	6.26	-1.59	4.05	-0.70	1.35	SK	1993
Summary	-0.59	7.25	-0.33	5.94	-0.17	0.73	SK	20293

T-VALUE	-11.54	THRESHOLD	1.64
WILCOXON	-8.67	THRESHOLD	1.64

TABLE A-8. SINGLE-PROFILE HELICOPTER, C-BAND

DATA	MEAN	STDEV	MEDIAN	S3 NORM	SKEWNESS	KURTOSIS	TESTS FAILED	# SAMPLES
04101559	-2.02	7.10	-2.25	7.24	-0.06	-0.14		3182
04101859	0.70	5.91	0.75	5.49	0.05	1.65	K	1202
04291259	-0.10	2.74	0.44	2.05	-1.26	1.77	SK	1510
04291459	1.10	3.37	1.42	3.86	-0.02	0.30	K	1451
04291759	0.76	9.06	2.52	8.48	-0.57	-0.47	SK	2933
04301259	-2.30	6.81	-1.41	4.56	-0.65	1.19	SK	2559
05021559	4.24	4.99	3.79	6.49	0.01	-0.88	K	1107
05031600	-5.10	8.87	-4.16	8.59	0.02	0.47	K	3482
05041159	0.25	4.35	-1.12	1.70	1.72	3.55	SK	2208
05041459	-3.99	4.54	-3.17	2.72	-0.17	3.05	SK	1851
05041959	-3.46	7.16	-1.65	4.62	-0.65	1.96	SK	2150
Summary	-1.49	7.20	-1.17	5.53	-0.41	1.07	SK	23635

T-VALUE	-31.75	THRESHOLD	1.64
WILCOXON	-29.48	THRESHOLD	1.64

TABLE A-9. SINGLE-PROFILE HELICOPTER, X-BAND

DATA	MEAN	STDEV	MEDIAN	S3 NORM	SKEWNESS	KURTOSIS	TESTS FAILED	# SAMPLES
04101559	3.56	8.87	3.50	8.29	-0.13	0.16	S	2348
04101859	-1.80	9.44	-2.79	8.56	0.46	0.54	SK	887
04291259	-1.70	3.03	-1.24	2.16	-0.20	2.46	SK	1408
04291459	-1.63	6.48	-0.60	3.94	-0.90	3.24	SK	1441
04291759	-1.14	7.25	-0.75	6.69	-0.32	0.32	SK	2771
04301259	1.69	9.78	-0.24	8.84	0.45	0.60	SK	2473
05021559	-3.44	6.95	-2.53	4.38	0.09	3.21	K	1114
05031600	-1.39	7.37	-0.35	5.64	-0.45	1.05	SK	3146
05041159	-1.51	3.13	-1.14	2.09	-0.32	2.45	SK	1974
05041459	-3.12	5.42	-2.99	4.26	-0.14	1.77	SK	1702
05041959	0.00	6.76	-0.25	5.66	-0.16	1.03	SK	2074
Summary	-0.63	7.47	-0.86	5.51	0.24	1.76	SK	21338

T-VALUE	-12.31	THRESHOLD	1.64
WILCOXON	-18.34	THRESHOLD	1.64

TABLE A-10. RANGE-DEPENDENT HELICOPTER, S-BAND

DATA	MEAN	STDEV	MEDIAN	S3 NORM	SKEWNESS	KURTOSIS	TESTS FAILED	# SAMPLES
04101559	3.73	4.21	4.38	3.26	-0.50	0.61	SK	2086
04101859	1.78	5.49	3.01	6.02	-0.21	-0.03	S	861
04291259	-0.76	2.55	-1.23	2.37	0.28	0.05	S	1300
04291459	1.81	4.32	0.26	2.98	0.92	0.13	S	1229
04291759	2.23	8.04	2.60	9.17	0.05	-0.56	K	2252
04301259	-3.36	5.51	-2.63	5.85	-0.23	-0.12	S	2259
05021559	5.31	4.61	5.85	6.20	-0.14	-1.40	K	916
05031600	-5.22	6.98	-4.98	5.36	-0.03	0.75	K	2130
05041159	-1.81	2.57	-1.99	1.19	2.65	13.28	SK	1495
05041459	-1.87	3.67	-1.86	1.42	0.04	6.04	K	1206
05041959	-2.14	6.19	-1.73	3.78	-0.07	1.78	K	1471
Summary	-0.37	6.31	-1.05	5.16	-0.07	0.91	SK	17205

T-VALUE	-7.70	THRESHOLD	1.64
WILCOXON	-9.59	THRESHOLD	1.64

TABLE A-11. RANGE-DEPENDENT HELICOPTER, C-BAND

DATA	MEAN	STDEV	MEDIAN	S3 NORM	SKEWNESS	KURTOSIS	TESTS FAILED	# SAMPLES
04101559	-2.09	5.40	-1.51	5.05	-0.81	2.01	SK	2868
04101859	3.06	7.33	2.94	7.20	0.21	0.43	SK	1202
04291259	-1.65	2.89	-2.25	2.69	0.08	-0.06		1510
04291459	2.49	5.41	1.08	4.58	0.79	-0.15	S	1365
04291759	3.51	9.67	4.30	9.88	-0.01	-0.42	K	2669
04301259	0.89	9.06	0.33	7.44	-0.53	1.06	SK	2386
05021559	4.44	4.56	4.31	5.93	-0.11	-0.43	K	955
05031600	-6.23	6.25	-6.03	5.99	-0.20	0.71	SK	2492
05041159	-1.48	2.71	-2.05	1.18	1.97	5.97	SK	1752
05041459	-1.66	4.56	-1.89	1.41	0.40	2.53	SK	1453
05041959	-3.03	6.36	-1.76	3.48	-1.26	4.04	SK	1566
Summary	-0.54	7.28	-1.29	5.11	0.11	1.61	SK	20218

T-VALUE	-10.55	THRESHOLD	1.64
WILCOXON	-17.35	THRESHOLD	1.64

TABLE A-12. RANGE-DEPENDENT HELICOPTER, X-BAND

DATA	MEAN	STDEV	MEDIAN	S3 NORM	SKEWNESS	KURTOSIS	TESTS FAILED	# SAMPLES
04101559	0.71	7.36	1.12	6.72	-0.18	0.32	SK	2113
04101859	3.21	10.82	3.56	11.15	0.00	-0.24		887
04291259	-2.32	3.44	-2.59	2.80	0.09	3.20	K	1408
04291459	-1.70	5.28	-0.58	3.04	-1.59	3.84	SK	1359
04291759	1.62	9.01	1.68	9.55	-0.38	0.29	SK	2500
04301259	2.02	7.31	1.80	5.84	0.10	1.78	SK	2312
05021559	-4.05	7.11	-2.78	4.57	-0.34	1.74	SK	965
05031600	-1.57	6.20	-1.21	5.95	0.00	1.00	K	2200
05041159	-2.70	3.38	-2.82	3.22	0.75	2.96	SK	1597
05041459	-2.66	4.42	-1.79	2.87	-0.41	4.50	SK	1314
05041959	1.06	6.68	0.66	5.60	-0.04	0.70	K	1538
Summary	-0.33	7.13	-0.70	5.60	0.18	1.54	SK	18193

T-VALUE	-6.27	THRESHOLD	1.64
WILCOXON	-10.68	THRESHOLD	1.64

TABLE A-13. FREE SPACE, S-BAND

DATA	MEAN	STDEV	MEDIAN	S3 NORM	SKEWNESS	KURTOSIS	TESTS FAILED	# SAMPLES
04101559	2.52	4.82	3.90	3.97	-1.11	1.21	SK	2625
04101859	8.81	3.57	9.80	2.57	-1.26	1.78	SK	470
04111500	1.54	7.72	3.72	5.42	-1.56	2.83	SK	1473
04111700	-6.07	7.79	-5.76	8.26	-0.41	-0.38	SK	2316
04291459	-0.97	5.24	0.27	4.71	-0.95	0.65	SK	570
04291759	-1.60	8.12	0.10	8.19	-0.81	0.07	S	2506
05021559	-0.38	4.72	1.27	3.42	-1.31	1.30	SK	1030
05021759	2.28	4.51	3.59	3.04	-1.70	4.08	SK	2104
05031600	-0.97	8.71	-0.71	9.39	-0.34	-0.44	SK	3320
05041459	-9.92	8.44	-9.84	9.55	-0.11	-0.73	K	1571
05051459	-7.64	9.62	-5.87	11.76	-0.46	-1.06	SK	1135
05081055	-12.50	5.61	-11.40	5.44	-0.60	-0.31	S	838
05081459	-3.87	6.76	-2.69	7.17	-0.56	-0.35	SK	1453
05081759	-2.35	6.16	-1.20	5.85	-0.96	1.36	SK	1321
05111359	2.18	3.97	3.48	2.67	-1.35	1.77	SK	1677
05111759	3.41	3.78	4.27	2.65	-1.78	5.20	SK	1825
Summary	-1.45	8.11	0.61	7.07	-0.88	0.35	SK	26234

T-VALUE	-28.94	THRESHOLD	1.64
WILCOXON	-13.27	THRESHOLD	1.64

TABLE A-14. FREE SPACE, C-BAND

DATA	MEAN	STDEV	MEDIAN	S3 NORM	SKEWNESS	KURTOSIS	TESTS FAILED	# SAMPLES
04101559	0.35	5.61	0.90	5.29	-0.87	1.50	SK	3589
04101859	8.59	3.09	9.37	2.59	-0.98	0.97	SK	657
04111500	1.17	8.08	3.77	7.58	-0.95	0.34	SK	1251
04111700	-5.84	8.05	-5.01	9.17	-0.46	-0.55	SK	2484
04291459	1.15	4.98	2.45	4.38	-1.14	1.03	SK	645
04291759	-1.61	8.69	0.66	8.91	-0.72	-0.46	SK	2933
05021559	1.20	4.40	3.08	2.14	-1.81	3.44	SK	1085
05021759	-1.48	5.84	-0.40	4.40	-1.28	2.60	SK	2304
05031600	-1.72	8.83	-0.75	8.27	-0.47	-0.06	S	3792
05041459	-8.92	8.24	-9.12	9.06	-0.16	-0.67	SK	1817
05051459	-6.91	9.18	-6.22	12.08	-0.49	-0.94	SK	1219
05081055	-12.70	5.93	-11.93	5.83	-0.35	-0.49	SK	1034
05081459	0.92	5.49	2.33	4.05	-1.05	1.26	SK	1484
05081759	0.73	6.30	2.08	4.88	-0.85	0.63	SK	1422
05111359	0.27	5.32	1.19	4.56	-1.03	1.80	SK	1831
05111759	1.86	5.15	2.76	4.83	-0.82	0.80	SK	2032
Summary	-1.69	8.06	0.08	7.11	-0.80	0.26	SK	29579

T-VALUE	-35.99	THRESHOLD	1.64
WILCOXON	-20.40	THRESHOLD	1.64

TABLE A-15. FREE SPACE, X-BAND

DATA	MEAN	STDEV	MEDIAN	S3 NORM	SKEWNESS	KURTOSIS	TESTS FAILED	# SAMPLES
04101559	0.80	5.30	1.99	4.27	-1.05	1.44	SK	2646
04101859	-3.61	6.73	-2.50	6.39	-0.89	0.68	SK	483
04111500	3.29	5.58	4.34	4.50	-1.12	1.56	SK	1255
04111700	-0.08	6.36	1.73	5.40	-0.98	0.38	SK	2344
04291459	-3.66	6.11	-2.01	5.13	-1.23	1.21	SK	632
04291759	-0.24	5.41	1.08	4.54	-1.10	1.14	SK	2771
05021559	-3.53	5.69	-2.66	5.62	-1.10	1.33	SK	1094
05021759	-3.65	5.37	-2.39	4.84	-1.04	0.89	SK	2177
05031600	3.11	6.52	4.71	5.28	-1.06	0.69	SK	3433
05041459	-3.35	6.90	-1.83	7.72	-0.74	-0.23	S	1676
05051459	-4.60	7.41	-2.41	7.62	-0.63	-0.82	SK	1134
05081055	-7.12	5.57	-6.25	5.46	-0.54	-0.37	SK	897
05081459	-1.93	6.91	-0.60	7.67	-0.69	-0.36	SK	1454
05081759	0.80	5.36	2.34	4.27	-1.26	1.67	SK	1404
05111359	-1.13	5.40	0.19	4.50	-1.37	2.32	SK	1809
05111759	-1.43	5.46	-0.03	4.72	-1.12	1.16	SK	2038
Summary	-0.87	6.52	0.46	5.81	-0.80	0.46	SK	27247

T-VALUE	-21.97	THRESHOLD	1.64
WILCOXON	-8.01	THRESHOLD	1.64

TABLE A-16. 4/3 EARTH, S-BAND

DATA	MEAN	STDEV	MEDIAN	S3 NORM	SKEWNESS	KURTOSIS	TESTS FAILED	# SAMPLES
04101559	32.04	18.79	30.42	25.48	0.05	-1.23	K	2625
04101859	26.91	7.41	25.78	7.35	0.41	-0.64	SK	861
04111500	14.89	10.11	15.02	14.43	-0.00	-1.54	K	1534
04111700	18.07	15.43	11.43	15.91	0.25	-1.70	SK	2316
04111959	5.40	4.33	4.29	4.26	0.85	-0.01	S	1500
04291259	4.47	4.19	3.88	4.94	0.34	-0.87	SK	1300
04291459	11.26	11.25	8.36	12.32	0.55	-0.97	SK	1305
04291759	28.56	18.45	31.37	21.57	0.54	0.03	S	2506
04301259	30.71	22.47	24.93	30.05	0.27	-1.28	SK	2408
05021559	11.41	9.16	10.80	10.97	0.30	-0.97	SK	1281
05021759	26.04	18.21	24.18	23.24	0.08	-1.27	K	2104
05031600	47.24	35.52	53.28	51.40	-0.10	-1.56	SK	3308
05041159	10.31	8.94	8.20	9.07	0.84	0.08	S	1919
05041459	7.97	10.18	4.53	6.09	1.60	1.70	SK	1593
05041959	24.12	20.12	21.74	26.94	0.30	-1.41	SK	2021
05051459	11.67	8.20	12.55	8.82	0.08	-0.74	K	1778
05081055	16.42	12.36	15.46	14.24	0.29	-0.96	SK	2071
05081459	23.40	18.42	25.44	27.17	-0.03	-1.64	K	2118
05081759	22.44	18.03	17.15	23.30	0.25	-1.40	SK	2025
05111359	26.54	17.60	26.22	21.98	0.20	-1.00	SK	2064
05111759	33.80	21.44	34.49	27.75	-0.02	-1.22	K	2159
Summary	22.81	21.37	16.64	20.09	1.06	0.74	SK	40796

T-VALUE	215.63	THRESHOLD	1.64
WILCOXON	170.77	THRESHOLD	1.64

TABLE A-17. 4/3 EARTH, C-BAND

DATA	MEAN	STDEV	MEDIAN	S3 NORM	SKEWNESS	KURTOSIS	TESTS FAILED	# SAMPLES
04101559	30.26	24.28	27.26	31.32	0.17	-1.26	SK	3589
04101859	25.56	8.91	25.68	9.52	-0.05	-0.40	K	1202
04111500	17.13	9.22	18.19	12.27	-0.17	-1.31	SK	1328
04111700	19.80	17.35	10.62	16.68	0.20	-1.74	SK	2484
04111959	6.45	5.05	5.50	6.24	0.29	-0.97	SK	1548
04291259	5.79	5.30	5.13	6.34	0.20	-1.02	SK	1510
04291459	11.82	12.29	9.06	13.48	0.45	-1.01	SK	1451
04291759	31.02	19.35	34.32	21.25	0.27	-0.16	S	2933
04301259	31.77	25.74	32.03	31.12	0.20	-0.86	SK	2559
05021559	12.23	10.44	11.44	13.63	0.23	-1.11	SK	1372
05021759	22.98	19.97	26.14	26.08	-0.04	-1.15	K	2304
05031600	48.62	38.89	51.80	61.28	-0.04	-1.49	K	3773
05041159	10.95	9.27	9.99	9.43	0.59	-0.16	S	2208
05041459	9.24	10.31	6.50	7.68	1.44	1.51	SK	1851
05041959	25.16	21.70	19.78	27.17	0.26	-1.56	SK	2180
05051459	13.55	10.42	13.95	9.94	0.12	-0.44	SK	1949
05081055	18.14	12.49	19.26	15.04	0.10	-1.03	K	2333
05081459	27.86	22.06	28.15	31.79	0.08	-1.54	K	2166
05081759	24.95	19.04	21.48	25.41	0.21	-1.32	SK	2198
05111359	25.55	21.88	25.89	29.29	0.11	-1.12	SK	2246
05111759	33.90	25.14	32.96	31.65	0.06	-1.06	K	2427
Summary	23.95	23.39	17.72	22.26	1.02	0.74	SK	45611

T-VALUE	218.64	THRESHOLD	1.64
WILCOXON	174.91	THRESHOLD	1.64

TABLE A-18. 4/3 EARTH, X-BAND

DATA	MEAN	STDEV	MEDIAN	S3 NORM	SKEWNESS	KURTOSIS	TESTS FAILED	# SAMPLES
04101559	24.92	24.97	20.42	30.06	0.32	-1.07	SK	2646
04101859	6.88	12.32	4.32	11.28	0.63	-0.04	S	887
04111500	10.37	11.02	8.24	9.29	0.32	-0.38	SK	1320
04111700	17.45	17.52	10.06	15.89	0.34	-1.42	SK	2344
04111959	5.09	7.19	3.12	6.21	0.18	-0.34	SK	1507
04291259	3.46	6.53	2.27	6.29	0.12	-0.05		1408
04291459	3.22	10.25	2.38	8.48	0.01	0.22		1441
04291759	25.78	26.48	20.93	31.28	0.35	-1.09	SK	2771
04301259	23.28	26.29	18.64	30.92	0.38	-0.93	SK	2473
05021559	1.25	10.36	-0.70	8.16	0.47	0.32	SK	1376
05021759	13.69	19.10	10.60	21.31	0.40	-0.94	SK	2177
05031600	48.89	38.28	45.22	53.41	0.12	-1.42	SK	3423
05041159	9.74	10.41	8.94	12.62	0.10	-0.74	K	1974
05041459	6.75	9.04	4.97	8.03	0.89	1.11	SK	1702
05041959	21.31	21.44	15.27	23.50	0.44	-1.06	SK	2101
05051459	8.96	12.84	9.08	14.82	-0.04	-0.65	K	1788
05081055	14.01	16.19	12.99	18.96	0.19	-0.86	SK	2142
05081459	14.07	17.59	10.36	15.11	0.72	-0.06	S	2116
05081759	18.09	19.10	15.85	21.99	0.29	-0.83	SK	2128
05111359	17.15	21.18	13.18	23.65	0.40	-0.84	SK	2205
05111759	23.73	26.00	18.65	30.65	0.35	-1.06	SK	2399
Summary	17.87	24.08	10.46	17.78	1.28	1.58	SK	42328

T-VALUE	152.64	THRESHOLD	1.64
WILCOXON	135.01	THRESHOLD	1.64

DISTRIBUTION

CD Copies

DOD ACTIVITIES (CONUS)

ATTN CODE A76
(TECHNICAL LIBRARY) 1
COMMANDING OFFICER
CSSDD NSWC
6703 W HIGHWAY 98
PANAMA CITY FL 32407-7001

DEFENSE TECH INFORMATION CTR 2
8725 JOHN J KINGMAN RD
SUITE 0944
FORT BELVOIR VA 22060-6218

ATTN N765 1
OFFICE OF CHIEF OF NAVAL OPERATIONS
THE PENTAGON RM 4C510
DEPARTMENT OF THE NAVY
WACHINGTON DC 20350-2000

ATTN CODE ONR313 (POLLOCK) 1
CODE ONR322 (FEREK) 1
CODE ONR351 (GRAFF) 1
CODE ONR353 (BELEN) 1
OFFICE OF NAVAL RESEARCH
800 N QUINCY ST BALLSTON TOWER ONE
ARLINGTON VA 22217-5660

ATTN CODE 543 (ROGERS) 1
CODE 543 (WAGNER) 1
COMMANDING OFFICER
SPAWARSYSCEN SAN DIEGO
53560 HULL ST
SAN DIEGO CA 92152-5001

ATTN PMS426 (HAGGERTY) 1
COMMANDER
NAVAL SEA SYSTEMS COMMAND
1333 ISAAC HULL AVE SE, STOP 2318
WASHINGTON NAVY YARD DC 20376-2318

ATTN CODE MR/DS (DAVIDSON) 1
NAVAL POST GRADUATE SCHOOL
DEPARTMENT OF METEOROLOGY
MONTEREY CA 93943

CD Copies

ATTN CODE PMS456 (RIVERA) 1
NAVAL SEA SYSTEMS COMMAND
1333 ISAAC HULL AVE SE, STOP 2320
WASHINGTON NAVY YARD DC 20376-2320

ATTN CODE N962C2 (MILLMAN) 1
THE OCEANOGRAPHER OF THE NAVY
UNITED STATES NAVAL OBSERVATORY
3450 MASSACHUSETTS AVE, NW
BUILDING ONE
WASHINGTON DC 20392-5421

ATTN CODE PMW155 (PIWOWAR) 1
SPACE AND NAVAL WARFARE SYSTEMS
COMMAND
METEOROLOGY AND OCEANOGRAPHY
SYSTEMS
4301 PACIFIC HIGHWAY, BUILDING OT-1
SAN DIEGO CA 92110-3127

NON-DOD ACTIVITIES (CONUS)

ATTN DOCKERY 1
NEWKIRK 1
JOHNS HOPKINS UNVERSITY
APPLIED PHYSICS LABORATORY
JOHNS HOPKINS RD
BALTIMORE MD 20723-6099

ATTN R/ETL6 (FAIRALL) 1
NOAA ENVIRONMENTAL TECHNOLOGY
LABORATORY
325 BROADWAY
BOULDER CO 80305

THE CNA CORPORATION 1
P O BOX 16268
ALEXANDRIA VA 22302-0268

DISTRIBUTION (CONTINUED)

CD Copies

INTERNAL

B05S	(STATON)	1
B60	(TECHNICAL LIBRARY)	3
G23	(BIBEL)	1
T		1
T40		1
T406	(HORMAN)	1
T41		1
T41	(KEENER)	1
T41	(PAWLAK)	8
T42		1
T44		1
T44	(WISS)	1
T44	(NGUYEN)	1
T44	(STAPLETON)	1
T45		1


NAVSEA
DAHLGREN
Surface Warfare Center Division